



Published in final edited form as:

Acta Biomater. 2019 May ; 90: 122–131. doi:10.1016/j.actbio.2019.04.004.

72-Hour In Vivo Evaluation of Nitric Oxide Generating Artificial Lung Gas Exchange Fibers in Sheep

Angela Lai¹, Caitlin T. Demarest¹, Chi Chi Do-Nguyen¹, Rei Ukita¹, David J. Skoog¹, Neil M. Carleton¹, Kagya A. Amoako², Patrick J. Montoya³, and Keith E. Cook¹

¹Carnegie Mellon University

²University of New Haven

³MedArray, Inc

Abstract

The large, densely packed artificial surface area of artificial lungs results in rapid clotting and device failure. Surface generated nitric oxide (NO) can be used to reduce platelet activation and coagulation on gas exchange fibers, while not inducing patient bleeding due to its short half-life in blood. To generate NO, artificial lungs can be manufactured with PDMS hollow fibers embedded with copper nanoparticles (Cu NP) and supplied with an infusion of the NO donor S-nitroso-N-acetyl-penicillamine (SNAP). The SNAP reacts with Cu NP to generate NO. This study investigates clot formation and gas exchange performance of artificial lungs with either NO-generating Cu-PDMS or standard polymethylpentene (PMP) fibers. One miniature artificial lung (MAL) made with 10 wt% Cu-PDMS hollow fibers and one PMP control MAL were attached to sheep in parallel in a veno-venous extracorporeal membrane oxygenation circuit (n = 8). Blood flow through each device was set at 300 mL/min, and each device received a SNAP infusion of 0.12 $\mu\text{mol}/\text{min}$. The ACT was between 110–180s in all cases. Blood flow resistance was calculated as a measure of clot formation on the fiber bundle. Gas exchange experiments comparing the two groups were conducted every 24 hours at blood flow rates of 300 and 600 mL/min. Devices were removed once the resistance reached 3x baseline (failure) or following 72 hours. All devices were imaged using scanning electron microscopy (SEM) at the inlet, outlet, and middle of the fiber bundle. The Cu-PDMS NO generating MALs had a significantly smaller increase in resistance compared to the control devices. Resistance rose from 26 ± 8 and 23 ± 5 in the control and Cu-PDMS devices, respectively, to 35 ± 8 mmHg/(mL/min) and 72 ± 23 mmHg/(mL/min) at the end of each experiment. The resistance and SEM imaging of fiber surfaces demonstrate lower clot formation on Cu-PDMS fibers. Although not statistically significant,

Corresponding Author: Angela Lai, **Telephone number:** 1 857 373 9177, **Fax Number:** 412 268 3025, angelala@andrew.cmu.edu, **Postal address:** 5000 Forbes Ave., 4th Floor Scott Hall, Pittsburgh PA, 15213.

Publisher's Disclaimer: This is a PDF file of an unedited manuscript that has been accepted for publication. As a service to our customers we are providing this early version of the manuscript. The manuscript will undergo copyediting, typesetting, and review of the resulting proof before it is published in its final citable form. Please note that during the production process errors may be discovered which could affect the content, and all legal disclaimers that apply to the journal pertain.

Data Availability

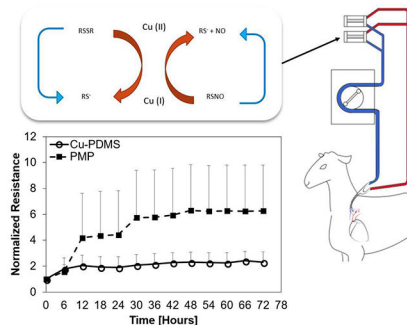
The raw, unprocessed data from this study is available and linked on the Mendeley Database under doi:10.17632/2cz2str9r4.1

Disclosure

There are zero conflicts of interest between the authors and this study.

oxygen transfer for the Cu-PDMS MALs was 13.3% less than the control at 600 mL/min blood flow rate. Future *in vivo* studies with larger Cu-PDMS devices are needed to define gas exchange capabilities and anticoagulant activity over a long-term study at clinically relevant ACTs.

Graphical Abstract



Keywords

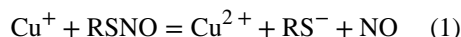
artificial lung; nitric oxide; oxygenator; coagulation; anti-platelet

1. Introduction

More than 200 million blood contacting medical devices are being used worldwide, with most using the same clinical materials available since the 1950s [1]. To this day, the problem that still persists is early thrombotic formation on blood contacting surfaces leading to early device failure and patient complications. Clot formation in artificial lungs and oxygenators is especially difficult to prevent due to the large, relatively dense, gas exchange membrane surface area. In these devices, clot formation leads to decreased gas exchange efficiency, high blood flow resistance and shear stresses, and risk of thromboembolism. This ultimately requires device replacement after 1–4 weeks of use, despite the use of systemic anticoagulants and surface coatings [2–6]. These anticoagulants also create a significant risk of bleeding complications to the patient, with 30% to 60% of patients having a significant bleeding event [7–10].

One potential means of slowing device failure without increasing the risk of bleeding is to create device-localized anticoagulation via biomaterial-based surface nitric oxide flux. Nitric oxide (NO) is an uncharged lipophilic messenger molecule in vertebrates, regulating many processes from blood flow, neural communication, and, of most interest in this study, thrombosis. This molecule is commonly used as an inhaled therapy to cause selective pulmonary vasodilation as in the case of emergency treatment of heart attack. In the field of artificial lungs, NO has been delivered via sweep gas or catalytically generated by copper containing materials contacting blood [11–17]. This approach mimics the natural endothelium, with NO fluxes into the blood ranging between $0.5\text{--}4 \times 10^{-10} \text{ mol cm}^{-2} \text{ min}^{-1}$ [18,19]. NO delivery has also been achieved with NO-donors that degrade over time to release the NO or with a catalyst that accelerates their decomposition. S-nitrosothiols, a NO-donor defined by a molecular bond between a thiol and nitric oxide, is a widely employed

donor due to its biocompatibility. Naturally occurring S-nitrosothiols are found in humans and other species, in the forms of S-nitroso-L-glutathione (GSNO) and S-nitroso-L-cysteine (CysNO). NO release from S-nitrosothiols can be catalyzed by heat, UV light, transition metals, and ascorbate. For blood bearing devices, Cu can be incorporated into polymeric surfaces easily and used to decompose S-nitrosothiols in a predetermined area. When used this way, Cu can cycle in a reduction-oxidation reaction seen in equations (1) and (2), where RSNO, RS⁻, and RSSR represent a S-nitrosothiol, thiolate anion, and disulfide, respectively.



As a stoichiometric reaction, the rate of NO release can be controlled with the availability of NO donor and how much Cu is exposed to the donor. This reduction-oxidation reaction can cycle indefinitely if there is a supply of the NO donor.

Previous studies have explored NO release with a copper catalyst with two types of experiments. Firstly, this technique has been applied to oxygenators by using silicone hollow fibers with incorporated Cu particles (Cu-PDMS) [13]. Surface expression of Cu had been demonstrated previously to be linearly related to NO flux achieved [12], ranging from plain PDMS with $0.16 \pm .34 \times 10^{-10} \text{ mol cm}^{-2} \text{ min}^{-1}$ to $5.35 \pm 0.74 \times 10^{-10} \text{ mol cm}^{-2} \text{ min}^{-1}$ with 10 wt% of Cu. This leads to clotting time increasing from 80 ± 13 seconds with pure PDMS to 338 ± 44 seconds with Cu-PDMS. These Cu-PDMS hollow fibers have been tested in miniature artificial lungs (MALs) for 4 hours in a pumpless arterio-venous rabbit model, demonstrating reduced platelet adhesion, clot formation, and occlusion [13,20]. Secondly, NO release or catalytic generation from simple coated catheters and grafts has also been investigated on a longer time scale, from 1 – 9 days, using *in vivo* lapine and ovine models, which demonstrated reduced clot formation [18,21]. However, NO releasing and generating surfaces have not yet been examined *in vivo* in the densely packed surfaces of artificial lungs for durations longer than 4 hours, nor in a large animal model, a significantly more challenging application.

The goal of this study was to compare the ability of 10 wt% Cu-PDMS fibers to the clinical standard fiber, polymethylpentene (PMP), to slow clot formation in a longer 72-hour experiment. A sheep model of veno-venous extracorporeal membrane oxygenation (ECMO) was used. The 10 wt% Cu concentration was chosen based on previous work that demonstrated significant reduction in clot formation during 4 hr. *in vivo* studies [12,13]. To accelerate clotting, normal clotting times were maintained rather than the clinical clotting times common to ECMO. Furthermore, the ECMO circuits for the present study utilized two small (0.05 m^2) artificial lungs in parallel such that both devices face the same blood conditions at all times. This conservative, head-to-head testing method reduces the influence of animal to animal variability on results, giving a clear answer as to which fiber material

clots more quickly. However, it does not allow one to attribute systemic changes in hematology to a specific device. Device blood flow resistance was used as measures of device performance and failure, and oxygen transfer and serum copper content were used to assess potential downsides of using Cu-PDMS fibers rather than PMP.

2. Materials and Methods

2.1 Nitric Oxide Generating Device and Circuit Components

Two types of artificial lung were tested in parallel. The first type used polymethylpentene (PMP) hollow fibers (Oxyplus, Membrana, Germany), and the second type used custom-made Cu-PDMS fibers. Cu-PDMS hollow fibers were made using a proprietary two-part silicone formulation which incorporated 10 wt% of 50 nm Cu particles within the silicone (Medarray, Ann Arbor, MI). Energy dispersive x-ray detector (EDX) testing revealed $26\% \pm 0.8$ surface copper expression, shown in Figure 1. This is the active surface that would decompose circulating NO-donors that come in contact with the surface.

To characterize the release of NO using a NO-donor and the Cu-PDMS surface, a 1 cm length of Cu-PDMS hollow fiber was introduced into a 37°C, 1 μ M RSNO in a reaction chamber. Nitrogen sweep gas was bubbled through the chamber with phosphate buffered saline (PBS, pH = 7.34) at 37°C and carried NO gas to the chemiluminescence detection chamber in the Sievers Nitric Oxide Analyzer (NOA), model 280 (Boulder, CO) where the gas nitric oxide content was determined by measuring the peak flux. The resulting peak NO flux measured from 4 separate fibers of 1 cm length is $3 \pm 0 \times 10^{-10}$ mol cm⁻² min⁻¹[12,15,20,22].

Both types of fiber had an outer diameter of 380 μ m, and the wall thicknesses of the PMP and Cu-PDMS fibers were 90 μ m and 55 μ m respectively. These fibers were wound into a fiber bundle with packing density of 50%. The total surface area from the fiber bundle was 0.05 m² for both designs. For both device types, the fiber bundles were encased in cylindrical polyethylene terephthalate-glycol modified (PETG) housings (figure 2) and potted with silicone potting (Elastosil RT 625, Wacker, Germany). Polyurethane (WC-753, BJB Enterprises, USA) corners were added in the distal end of the blood inlet and outlet to reduce prime volume and stasis regions, as indicated by the labels in Figure 2c. Each device had a prime volume of 43 ± 2 mL. The entire circuit, consisting of the two devices in parallel, and 1/4" and 3/8" ID Tygon tubing had a prime volume of 300 mL and was sterilized using ethylene oxide before the surgical attachment.

2.2 Experimental Methods

All methods were approved by the Allegheny Health Network International Animal Care and Use Committee, in accordance to the National Institutes of Health Guide for the Care and Use of Laboratory Animals. Nine sets of devices were attached to five Montadale sheep with an average weight of 56 ± 2 kg (Shiloh Farms, USA). A transdermal fentanyl patch (75 – 100 μ g/h, n = 5) was given 12 hours before surgical incision to provide 72 hours of analgesia. Initial anesthesia was induced with 4 – 6 mg/kg propofol and then maintained with 1–5% inhaled isoflurane for the duration of surgery. Penicillin (40,000 U/kg) and

Enrofloxacin (5 mg/kg) were given every 72 and 24 hours, respectively. A beveled 24-inch long pressure tubing (Tru-Wave, Edwards Lifesciences, USA) was placed in the carotid artery for pressure monitoring and blood sampling. Lactated Ringer's solution was administered intravenously at a rate of 10 mL/kg/hr to maintain blood pressure stability.

Baseline arterial blood samples, including blood gases (pO_2 , sO_2 , pCO_2 , pH, total hemoglobin) and hematology (platelet count, white blood cell count, methemoglobin, activated clotting time, plasma free hemoglobin, and hematocrit), were taken immediately after the arterial line was attached. A bolus of heparin (200 U/kg) was administered arterially, and the Avalon Elite Bi-Caval Dual Lumen Catheter (Maquet, NJ) was placed in the jugular vein. The circuit was primed with a solution of 1% albumin in saline for 15 minutes prior to the experiment to slow early protein adsorption and clot formation in a similar fashion as previous work [23,24]. The prime solution was also dosed with methylprednisolone sodium succinate (30 mg/kg) and heparin (100 U) before attachment. This circuit contained all the tubing and connectors but not the artificial lungs. For safety and simplicity, these devices weren't attached until the sheep was moved and stabilized in long-term housing. The circuit flow was started at 600 mL/min with a roller pump and monitored with an ultrasonic flow probe and flow meter (Transonic T402 Ithaca, NY).

After circuit attachment, the sheep were moved to a custom-built stanchion, recovered, and moved to long-term housing. One PMP device and one Cu-PDMS device were attached in parallel within the circuit after six hours of initial circuit attachment (figure 3). Each device received a separate continuous infusion of a NO donor, S-Nitroso-N-acetyl-DL-penicillamine (SNAP) (Sigma Aldrich, USA), at a rate of 0.48 $\mu\text{mol}/\text{min}$ at the inlet to replace any lost NO donors in blood. This infusion rate was based on a previous *in vivo* study that used a miniature artificial lung with the same MedArray Cu-PDMS fibers as a NO generating surface [13]. Throughout the duration of the experiment, the pump speed was adjusted to maintain blood flow at 300 mL/min per device (approximately 5% of the cardiac output) [25,26]. Screw clamps were used at the outlet of each device to maintain even flow through both devices. This blood flow rate was chosen to match the blood flow velocity at a relatively low 2 L/min of blood flow through an adult Quadrox HMO 70000 with a 100 cm^2 frontal area, or 20 cm/min. Although gas transfer was not necessary in these normal sheep, room air was supplied as the sweep gas through each device at double the blood flow rate to mimic the sweep gas flow rates used in the clinic. The results would thus reflect any loss of NO transferred from the surface generated NO into the sweep gas phase. Once every 24 hours, the sweep gas was switched to 100% O_2 for gas exchange testing, while maintaining gas flow rates at twice the blood flow rates. The blood flow rates were set at 300 and 600 mL/min, and inlet and outlet blood samples were taken to perform blood gas analysis using an ABL800 Flex Analyzer (Radiometer, Brea, USA). Immediately after gas exchange testing, the gas inlet was reconnected to room air flowing at 600 mL/min, and the blood flow was returned to 300 mL/min.

2.3 Data Acquisition and Blood Sampling

After devices were first attached, the pressure drop and blood flow rate through for each device were immediately measured to calculate a baseline resistance. The pressure drop

across each device (P) was measured with pressure transducers (Transpac ® IV Monitoring Transducers, ICU Medical, USA) and the flow rate (Q) with a tubing flow probe (Transonic T402 Ithaca, NY, Ithaca NY). Each subsequent hour afterwards, the resistance was also calculated from pressure drop and blood flow rate. Additionally, arterial blood samples were taken immediately after device attachment to measure activated clotting time (ACT), HCT, platelet and WBC counts. After initial device attachment samples were taken, blood gas samples were taken every 3 hours, and platelet and WBC counts were taken every 12 hours. Blood-gas and plasma free hemoglobin samples were drawn into heparinized syringes, and platelet count samples were taken into 10% sodium citrate syringes. Arterial blood pH, pCO_2 , pO_2 , total hemoglobin, methHgb were measured with an ABL800 Flex Analyzer (Radiometer, Brea CA) every 6 hours. Plasma-free hemoglobin was measured with a spectrophotometer using the Cripps method [27], and total platelet and white blood cell counts were measured using a Z1 Coulter Counter (Beckman Coulter Electronics, Hialeah FL) every 12 hours. The ACT was measured every hour until stable (three hourly samples within 100–180 s) and then every 4–6 hours. ACT was measured with a Model 801 Hemochron Blood Coagulation System (International Technidyne Corp. Edison NJ). During the entire experiment, ACT was maintained between 100–180 s, and averaged at 150 ± 9 s for all experiments. It was unnecessary to infuse heparin in 7 of the 8 sets of circuits to maintain this range. In sheep 4, ACT dropped below 100s, and heparin was infused for a period of 30 hours. Mean arterial pressure and heart rate were monitored continuously on a patient monitor and recorded every hour to assess overall health as NO is a known vasodilator and could cause a blood pressure drop.

Devices were considered failed if the resistance reached three times the baseline resistance and were removed and replaced with a shunt tube or removed following 72 hours if failure did not occur. After the first set of devices were removed, a second set of devices, consisting of one PMP and one Cu-PDMS in parallel, was attached. The removed devices were immediately injected with 5 mL of heparin to prevent the stagnant blood from clotting and then rinsed with heparinized saline (2 U/mL) until the effluent was clear. These devices were then disassembled with the clear housing carefully cut away to isolate the clot on the fiber bundle for imaging. The surface at the inlet, outlet, and middle of the fiber bundle were rinsed with saline until the effluent ran clear and then each sample was fixed in 2% glutaraldehyde (Electron Microscopy Sciences, USA). Small squares ($1.5 \text{ cm}^2 \times 1.5 \text{ cm}^2 \times 1.5 \text{ cm}^2$) from each fiber bundle were excised and dehydrated and sputter coated in platinum for scanning electron microscopy (SEM) imaging (Philips XL-30, Hillsboro Oregon) with the following settings: accelerating voltage 10 kV, beam size 3, and working distance 10 mm.

Sheep were euthanized at the end of the experiment using Fatal Plus (Vortech, USA) and necropsied for tissue samples from the liver and serum. Tissue samples and serum samples were then assayed for copper content with a quantitative colorimetric copper assay (DICU-250, Gentuar BioAssay Systems, USA). Blood samples were taken from two sheep without circuits attached for a negative control, using a gravity drip method and anticoagulated with a 1:9 ratio of acid-citrate-dextrose. Copper content was measured the same way as described above.

2.4 Statistical Analysis

Resistances were analyzed for devices that were attached 6 hours after circuit attachment. Device resistance was calculated as $R = P/Q$ every hour, where P is pressure drop across the device, and Q is blood flow through the device. Resistance data were then normalized to the percentage increase in resistance above the average of all baseline resistances. The normalized data is then averaged across 6-hour periods for statistical analysis and presentation. Devices that reached three times the baseline resistance for two consecutive hours before 72 hours were considered to have failed. Devices that fail are removed and thus have no further measure of resistance. For presentation and statistical analysis, the resistance of each device following failure was conservatively assumed to remain the same. This resistance value is less than the likely exponential increase in resistance that typically follows device failure and eliminates the misleading information when the device is censored from the graph thereafter. For statistical analysis, normalized resistances were compared across all devices with SPSS (IBM, Chicago USA) using a mixed model analysis with a Bonferroni-corrected confidence interval with each set as the subject variable, and time as the fixed, repeated-measure variable [28,29]. A p -value < 0.05 is regarded as significant.

Oxygen transfer was calculated with the following equation,

$$O_2 \text{ transfer rate} = kQ_b\Delta P + 1.34C_{Hb}Q_b\Delta S$$

With k as the solubility of O_2 in blood (3.56×10^{-5} mL O_2 /mL blood/mmHg), Q_b is the blood flow rate, C_{Hb} is the hemoglobin concentration, P is the difference in O_2 partial pressure and S is the difference in oxyhemoglobin saturation between the device inlet and outlet. Two analyses of gas transfer were performed. In the first, only paired data from the Cu-PDMS and PMP devices from the same time point were used to rule out variations in gas exchange due to varying inlet conditions. As both devices were in parallel, each would have experienced the same inlet conditions. In addition, to address potential variation in gas exchange due to clot formation on the fiber bundle, a separate analysis was performed using only the first set of gas exchange data from each device. The first gas exchange experiment is completed within 2 hours of attachment, at a point when clot formation on the fiber bundle should not yet affect gas exchange. The data from any device with a resistance increase of more than 5 mmHg/mL/min was excluded for analysis.

Differences between PMP and Cu-PDMS failure rates were analyzed using the Kaplan Meier method within SPSS. A t-test assuming unequal variances was used to analyze the difference between the platelet values at the start of the first and second sets of devices attached to each subject. Lastly, all hematology variables and blood pressure were averaged for each sheep over 6-hour blocks of time, and this data was used for statistical analysis. Graphs were created using Excel (Microsoft Inc. Redmond, WA).

3. Results

Five sheep had two sets of devices tested. One sheep accidentally decannulated due to inadequate cannula suturing and was euthanized at 14 hours. One set of devices was attached less than 6 hours after surgery and was outside of protocol and was not used. Thus, a total of 9 sets of devices were attached, and data from 8 were used for analysis. During testing, sheep mean arterial blood pressure and heart rate were stable and within normal ranges, averaging 91 ± 3 mmHg and 105 ± 3 bpm, respectively, from baseline to day 6. The methemoglobin levels remained at baseline values averaging $1.9 \pm 0.2\%$. The average ACT was 150 ± 10 s and did not vary significantly over the course of the experiment ($p=0.43$).

3.1 Coagulation and inflammation

Plasma free hemoglobin counts remained at baseline values throughout each experiment and did not vary significantly over all experiments ($p=0.58$). The average white blood cell count was $9 \pm 1 \times 10^3$ cells/ μ L at baseline, rose to $11 \pm 2 \times 10^3$ cells/ μ l on day two after circuit attachment, and fell back towards starting values by day three (figure 4). There was no response seen as a result of the second set of device attachment, perhaps due to the smaller change in surface area compared to the entire circuit and device attachment on day zero and some white cell exhaustion. There was a significant drop in platelets from baseline after the circuit was attached due to initial platelet adhesion to the oxygenators and circuit. However, platelet count returned towards baseline after day two, as seen in the minimum platelet count on day two at $149 * 10^3/\mu$ l increasing to $381 * 10^3/\mu$ l on day 5 (figure 4). There was no significant difference ($p = 0.977$) in the platelet counts or in the white blood cell counts ($p=0.787$) during the first and second set from a 2-tail student t-test.

3.2 Device Function

Blood flow resistance, measured in mmHg/mL/min, increased from BL to 72 hours for both cases; however, the control PMP devices exhibited significantly greater resistance than the Cu-PDMS devices which indicates more clot on the fiber bundle ($p<.001$) (figure 5). The failure curve (figure 6) shows greater longevity for Cu-PDMS devices than PMP devices, however, using a log-rank Kaplan Meier analysis this did not reach significance($p=.171$). The NO generation in the Cu-PDMS devices caused a marked reduction in clot formation and failure between the 12 to 36-hour range: by hour 36, 62.5% of control devices had failed, whereas only 12.5% of the Cu-PDMS devices had failed. At 72 hours, 87.5% of the control devices failed, while only 50% of the Cu-PDMS failed.

Table 1 provides the exact failure time of each set of paired devices. The first and second set of Cu-PDMS devices failed after an average of 40.5 ± 31 hours and 49.0 ± 13 hours respectively. For the PMP devices, the first set of devices lasted an average of 24.5 ± 27 hours before failing while the second set lasted an average of 32.3 ± 16 hours. There was significant variation between tests with a few obvious outliers in each group, as 12.5% of Cu-PDMS devices failed before 40 hours and 12.5% of PMP devices survived the entire 72 hours.

After the experiment, the fiber bundle removed from each device revealed that clot originated from the gas exchanging fibers or from the housing at the edge of the fiber bundle. All devices had clot on the outlet housing, but failed devices had more clot on the fiber bundle surface than on the housing. Figure 7 shows pictures of representative devices after failure (n = 7 PMP, n = 4 Cu-PDMS) or at 72 hours if they did not fail (n = 1 PMP, n = 4 Cu-PDMS).

Oxygen transfer measurements provided additional information on Cu-PDMS performance. Data examining day 1 devices were used. Average O₂ transfer of copper devices was 92 ± 17 mL O₂/min/m² and the average O₂ transfer of PMP devices was 106 ± 29 mL O₂/min/m² at a blood flow rate of 600 mL/min. Average O₂ transfer at 300 mL/min blood flow was 76 ± 11 mL O₂/min/m² for copper devices and was 91 ± 16 mL O₂/min/m² (Figure 8) (Table 2). Using a 2-tail student t-test, there was no significant difference between the Cu-PDMS and PMP gas exchange performance (p=0.65 and p=0.72, respectively). There was no significance because the control devices did not perform consistently better than the Cu-PDMS devices. In the following days, each subsequent oxygen transfer measurement was lower than the previous day's and can be seen in Table 2.

3.3 Sheep Necropsy and copper content

SEM images were taken to assess overall clot formation on gas exchanging hollow fiber surfaces as well as on the non-gas exchanging, weaving fibers that are used to tie the fibers together. While clot filled both sides of failed Cu-PDMS and control devices, the gas exchanging fibers in these devices exhibited different surface fouling. The SEM images in figure 9 were chosen as representative images since they were typical for each case. As seen in figure 9, there was more protein deposition on the PMP control hollow fibers than there were on the Cu-PDMS hollow fibers. However, weaving fibers in both cases were covered with substantial clot.

Organ and serum copper concentrations of each subject were measured at the end of the experiment using the DICU 250 quantitative colorimetric kit (n = 5). Copper content measured in serum averaged 233.72 ± 69 µg/dL, greater than normal average sheep copper content of 90–160 µg/dL. Final liver copper content averaged 31 ± 11 µg/g, within the normal levels of 18–87 mcg/g) [30].

4. Discussion

This study assessed a Cu-PDMS NO generating hollow fiber device in a short-term, large animal biocompatibility experiment. The results indicate that catalytic generation of NO at $3 \pm 0 \times 10^{-10}$ mol cm⁻² min⁻¹ by Cu-PDMS fibers reduces clot formation when compared to standard PMP fibers. However, this benefit is not consistent across each study. The Cu-PDMS did not affect sheep health and hematology in this setting nor did it create a statistically significant reduction in gas exchange efficiency.

4.1 Clot Formation

As hypothesized, NO generation slowed clot formation, resulting in the reduced blood flow resistance increases, failure rates, gross thrombus (Figure 7), and thrombus observed via

SEM. This positive effect was most pronounced in the first 36–40 hours of testing but waned thereafter in a number of the Cu-PDMS devices (Figure 6). This suggests that while the NO flux provides anticoagulation, this effect was eventually overcome by surface generation of clotting factors. After 36–40 hours, the accumulation of fibrin on the devices along with the increasing sheep platelet count was too much for NO generation to overcome. Furthermore, although Cu-PDMS devices had slower clot formation, on average, the results were not consistent, 12.5% of Cu-PDMS devices failed before 40 hours and 12.5% of PMP devices survived the entire 72 hours. No obvious differences in platelet counts or ACT could explain the cause of this outlying behavior. The early Cu-PDMS failure occurred with a platelet count of 382×10^3 cells/ μL and ACT of 144 s vs. an average of $275 \pm 50 \times 10^3$ cells/ μL and 150 s respectively, in the devices with more typical function. The slower clot forming PMP device had a platelet count of 246×10^3 cells/ μL and ACT of 157 s. This suggests other causes, such as greater concentrations of coagulation factors or device manufacturing variability (see section 4.4).

Furthermore, the NO also caused significant reductions of fiber clot on the gas exchange fibers on SEM. However, there was ubiquitous clot formation on the polypropylene warp fibers of both Cu-PDMS and PMP bundles. These are the non-gas exchanging fibers that are knitted into the fiber every 1 cm to hold the fiber mat together (Figure 9). Because this requires multiple, small fiber strands, this area has multiple small interstices and a high surface area to blood volume ratio, leading to efficient generation of procoagulants. Moreover, there is no blood flow through these interstices to wash activated procoagulants from the surface, and these fibers do not contain the copper catalyst. As a result of stagnation and lack of NO flux, these fibers clot rapidly.

4.2 Improving the Anticoagulant Function of NO Generating Fibers

In this study, the anticoagulation function of NO was not as consistently positive as during previous, short-term studies [13,15,31]. One potential cause of this may have been the low average ACTs (150s) in this study. Nitric oxide does nothing to prevent surface adsorption of plasma proteins such as fibrinogen and the contact system of the intrinsic branch of the coagulation cascade. In fact, there is evidence that NO can enhance fibrinogen adsorption [15,20,32,33]. Platelet adhesion to fibrinogen causes platelet activation, while protein adsorption and activation of the intrinsic branch of the coagulation cascade generates thrombin that can further enhance platelet activation [32]. Because of this, anti-adsorptive surface coatings could be combined with NO generation to limit the amount of platelet agonists present and thus enhance the ability of NO to inhibit platelets. Previous research has shown that anti-adsorptive surface coatings work synergistically with NO surface flux to further decrease platelet surface adhesion [13,14]. However, these studies created NO flux by delivering NO within the oxygenating gas of the gas exchanger. For catalytic NO generation, surface coatings could potentially reduce Cu interactions with SNAP and thus reduce NO flux rates.

NO generation from fibers should also be optimized to improve its function. First, the ideal rate of NO donor infusion is not known. The infusion rate for this study, $0.48 \mu\text{mol}/\text{min}$, matches that provided when testing a similar but slightly larger surface area artificial lung

during a 4-hr rabbit study [13]. It is unknown if this rate of delivery generates the maximum NO flux without also causing systemic vasodilation and hypotension or elevated metHb. Lastly, much of the ECMO circuit wasn't coated with Cu nanoparticles in this study. In future studies, the entire ECMO circuit could be coated with Cu nanoparticles, including the warp weaving fibers, to catalytically generate NO at every surface.

4.3 Side-Effects – Oxygen Transfer and Serum Copper

A secondary goal of this study was to examine if there are differences in the gas transfer efficiency of the two fiber types due specifically to differences in fiber wall oxygen permeability. Isolating the role of the permeability requires significant control over the other variables affecting oxygen transfer in these devices. In addition to fiber wall oxygen permeability, oxygen transfer in any artificial lung fiber bundle is a function of blood composition and chemistry, blood flow velocity, and fiber bundle geometry [34]. During a long-term study, clot formation will also reduce gas exchange by reducing the amount of fiber exposed to flowing blood and changing blood flow patterns and velocity within the open portions of the fiber bundle. Therefore, to isolate the effect of fiber wall permeability, the study sought to do the following:

1. Each device was constructed with the same methodology in order to construct fiber bundles with identical geometries.
2. Blood inlet chemistry and composition is the same for each paired PMP and Cu-PDMS fiber bundle, and
3. Devices were only analyzed if their initial resistance was very close to the typical starting resistance for these devices (15 ± 5 mmHg/mL/min), to eliminate outliers with significant clot formation.

Following these methods, results of this analysis indicate a small, statistically insignificant reduction in gas exchange efficiency with the Cu-PDMS fibers when compared to the PMP fibers. Examination of each specific pair of devices showed that there was no consistent trend in superior gas exchange for the PMP or Cu-PDMS fibers.

Although this suggests similar gas exchange, these results were confounded by variations in gas exchange efficiency within both the Cu-PDMS and PMP groups. These differences cannot be explained by differences in blood inlet chemistry or composition. Each paired device was tested at the same inlet conditions, pO_2 at 45 ± 4 mmHg, sO_2 at $65 \pm 7\%$, and hematocrit $21 \pm 3\%$ for all samples. If, for example, there is a lower than normal inlet saturation, this would result in increased gas exchange for *both* devices rather than an abnormally low or high gas exchange in one. Thus, inlet blood conditions are not the source of variation, and studies of these devices under controlled inlet conditions would change the extent of gas exchange, but not the inconsistency regarding which fiber delivered better oxygenation. Clot formation is also not the source, as this has been controlled for the results in Figure 8. Thus, the cause of this variation is likely differences in device construction. While each of the miniature artificial lungs were produced with the same methodology, they are hand-made and likely to vary by some degree. This is common in prototype artificial lungs [24,35]. Fiber bundle frontal areas and path lengths, potting depths, and/or the

percentage of fibers open for gas flow can vary slightly in these devices. Furthermore, blood flow can shunt around the fiber bundle to some degree. These differences affect blood flow patterns and the amount of fiber surface area available for gas exchange. The cause of these differences is unlikely varying amounts of Cu present in the fibers, as the distribution of Cu in the membrane was found to be homogenous and largely uniform in the SEM images from the sampled Cu-PDMS fibers.

In addition to assessing the negative effects on gas exchange, care must also be taken that leaching copper does not lead to systemic toxicity during long-term support. Copper toxicity manifests mainly as liver cirrhosis and damage, as non-reabsorbed copper is mainly excreted in bile produced by the liver. Mammal blood has endogenous copper that is mainly bound to albumin and transcuprein as a reservoir, before it is transported to the liver [36]. The kidney also receives copper from the blood and absorption from the gut and may have increased copper concentrations as a result of enhanced tubular reabsorption of circulating copper. Therefore, the copper toxicity exhibits itself as liver cirrhosis first and then with episodes of hemolysis and damage to renal tubules, the brain, and other organs [37,38]. In sheep specifically, the tolerance for copper is low and some are unable to increase biliary copper excretion in response to increased copper intake, making it a conservative model [39]. In this study, copper concentration taken from the liver remained low, $31 \pm 11 \mu\text{g/g}$ of tissue compared to averages seen in sheep which range from 18–87 $\mu\text{g/g}$ [40–43]. On the other hand, copper serum content was elevated above normal levels. Together, this suggests active leaching into the blood but no toxic build-up within the liver.

Although these results are positive, this device was undersized purposely so that systemic hematology would be less affected by the attached devices (see section 4.4). As a result, the hollow fiber surface area of this device is $1/26^{\text{th}}$ of a typical full-sized ECMO oxygenator. Therefore, it grossly underestimates the amount of copper that would leach using commercial oxygenators. Moreover, those devices are likely to be used for longer periods. Therefore, further long-term testing is also required to study Cu-PDMS biocompatibility.

4.4 Effect of Study Design and Test Devices on Clot Formation and Study Conclusions

The primary purpose of this study was to assess the relative thrombogenicity of NO generating fibers when compared to the clinical standard PMP fibers. Typically, *in vivo* studies are utilized to supply a source of fresh, coagulable blood. These studies are more realistic than *ex-vivo* studies using sampled or banked blood, as *ex-vivo* blood processing induces changes in coagulation factors, platelet function, and anticoagulation that change the coagulability of blood. To improve upon this, there are two types of *in vivo* studies that are typically run. In one type, the researcher seeks to perfectly recapitulate the clinical situation, such as testing a full-scale oxygenator in an adult-sized animal [35,44–46]. In another type, the animal is used solely as a source of fresh coagulable blood, which is pumped over a biomaterial to assess their interaction [13,18,33,47]. This is more accurate than an *ex-vivo* recirculation study with a fixed blood volume as the blood retains a more normal ability to coagulate. However, in these studies, the animal and circuit size do not always match that of the clinical situation, and the focus is, or should be, primarily on the local coagulation in the device or at the biomaterial surface, rather than systemic effects.

This study is of the latter type. Blood was pumped from the sheep and through both devices. The goal of the study design was to expose both types of fiber bundle materials to blood with the exact same characteristics, so that a true head to head comparison of their thrombogenicity could be made. The main advantage of this approach is that devices are tested under exactly the same conditions. Like humans, different sheep have different coagulation systems, leading to significant variations in clotting within medical devices. In this study design, if a sheep is highly procoagulant, for example, this is reflected in results for both of the paired PMP and Cu-PDMS fiber bundles. This reduces the effect of animal to animal variability on statistical analysis.

At the same time, this study design creates the potential for one device to affect the performance of the other device. If one device is highly procoagulant, this will lead to greater generation of circulating procoagulants that could accelerate failure for the paired device. To limit this effect during this study, devices were made to purposely have a small surface area and operate under a lower flow rate. A clinical ECMO oxygenator, such as the Maquet HMO 70000, has a 1.3 m² fiber bundle surface area that is 79% of the surface area of the oxygenator, and the oxygenator typically processes 33–67% of the cardiac output. This full-sized device also has a prime volume of 215 mL. Together, this means that the fiber bundle can cause marked derangements in systemic hematology, including generation of procoagulants and pro-inflammatory cytokines, platelet activation, and hemolysis. In this study, large (56 ± 2 kg) sheep used devices had 0.05 m² surface area fiber bundles, making up 77% of the total gas exchanger surface area, with flow rates that were 5–6% of cardiac output. The prime volume of this experimental device was 43 ± 2 mL. Thus, the effect on systemic hematology is small, as so is the effect of one device on the other.

Therefore, these results indicative of the relative thrombogenicity of the two fiber types, but not of clinical ECMO using these fibers. Extrapolation of these results to performance of full-scale oxygenators during clinical ECMO is unwise due to the size of the tested devices in this study, their relatively low flow rate, the use of two devices at one time, and the withholding of heparin anticoagulation and the resulting low ACT (150 ± 10 s). In particular, this latter condition created an aggressive test of the ability of NO to reduce clot formation. If heparin had been used to generate a more clinically applicable ACT of 180–220s, there would have been reduced thrombin formation and thus lower levels of platelet activation and fibrin formation. This would, in turn, increase the time to failure for each device. Therefore, to judge the true clinical impact of the technology, future studies will need to test full-scale devices in single animals with ACTs ranging from 180–220s.

Lastly, the effectiveness of NO generating surfaces will likely depend to some extent on the oxygenator design and, specifically, the extent of flow stagnation. If there are stagnation regions in an oxygenator, NO flux rates may be reduced by poor convection of SNAP to that surface. The specific ability of NO generation to elongate the useful lifetime of any device would, therefore, have to be evaluated on that specific device.

Conclusion

This study assessed the effect of Cu catalyzed NO generation on clot formation in a low-ACT, accelerated clot formation model of VV ECMO. This is the first study to investigate this effect in a long-term, large-animal model. The NO-generating, Cu-PDMS fibers significantly slowed clot formation and maintained fiber bundle patency. However, this effect was not consistent for each pair of devices tested. The effect of Cu on oxygen transfer was small but confounded by device to device variability. Leaching of copper lead to elevated copper serum content but no build-up in the liver. Future studies should investigate blood clotting and serum Cu levels in studies with full scale oxygenators and normal levels of heparin anticoagulation over a period of weeks.

Acknowledgements

This research is funded by the National Institutes of Health [2R01HL089043].

References

- [1]. Ratner BD, The catastrophe revisited: Blood compatibility in the 21st Century, *Biomaterials* 28 (2007) 5144–5147. doi:10.1016/j.biomaterials.2007.07.035. [PubMed: 17689608]
- [2]. Haneya A, Philipp A, Mueller T, Lubnow M, Pfeifer M, Zink W, Hilker M, Schmid C, Hirt S, Extracorporeal circulatory systems as a bridge to lung transplantation at remote transplant centers, *Ann. Thorac. Surg* 91 (2011) 250–255. doi:10.1016/j.athoracsur.2010.09.005. [PubMed: 21172523]
- [3]. Fischer S, Simon AR, Welte T, Hoepfer MM, Meyer A, Tessmann R, Gohrbandt B, Gottlieb J, Haverich A, Strueber M, Bridge to lung transplantation with the novel pumpless interventional lung assist device NovaLung, *J. Thorac. Cardiovasc. Surg* 131 (2006) 719–723. doi:10.1016/j.jtcvs.2005.10.050. [PubMed: 16515929]
- [4]. Strueber M, Hoepfer MM, Fischer S, Cypel M, Warnecke G, Gottlieb J, Pierre A, Welte T, Haverich A, Simon AR, Keshavjee S, Bridge to thoracic organ transplantation in patients with pulmonary arterial hypertension using a pumpless lung assist device, *Am. J. Transplant* 9 (2009) 853–857. doi:10.1111/j.1600-6143.2009.02549.x. [PubMed: 19344471]
- [5]. Maul TM, Massicotte PM, Wearden PD, ECMO Biocompatibility: Surface coatings, anticoagulation, and coagulation monitoring, in: *Extracorpor. Membr. Oxyg. - Adv. Ther.*, 2016: pp. 27–56.
- [6]. Camboni D, Philipp A, Arlt M, Pfeiffer M, Hilker M, Schmid C, First Experience With a Paracorporeal Artificial Lung In Humans, *ASAIO J* 55 (2009) 304–306. doi:10.1097/MAT.0b013e31819740a0. [PubMed: 19282751]
- [7]. N LM, Gary R, Seth L, Clive K, Hemorrhagic Complications of Anticoagulant Treatment, (2001). doi:10.1378/chest.119.1.
- [8]. Dalton HJ, Garcia-Filion P, Holubkov R, Moler FW, Shanley T, Heidemann S, Meert K, Berg R, Berger J, Carcillo J, Newth C, Harrison R, Doctor A, Rycus PT, Dean M, Jenkins T, Nicholson C, Association of bleeding and thrombosis with outcome in Extracorporeal Life Support, *Pediatr. Crit. Care Med* 16 (2015) 167–174. doi:10.1097/PCC.0000000000000317. Association. [PubMed: 25647124]
- [9]. Mazzeffi M, Greenwood J, Tanaka K, Menaker J, Rector R, Herr D, Kon Z, Lee J, Griffith B, Rajagopal K, Pham S, Bleeding, Transfusion, and Mortality on Extracorporeal Life Support: ECLS Working Group on Thrombosis and Hemostasis, *Ann. Thorac. Surg* 101 (2016) 682–689. doi:10.1016/j.athoracsur.2015.07.046. [PubMed: 26443879]
- [10]. Schmidt M, Stewart C, Bailey M, Nieszkowska A, Kelly J, Murphy L, Pilcher D, Cooper K, Scheinkestel C, Pellegrino V, Forrest P, Combes A, Hodgson C, Mechanical Ventilation Management During Extracorporeal Membrane Oxygenation for Acute Respiratory Distress

Syndrome: A Retrospective International Multicenter Study, *Intensive Care Med* 40 (2014) S10. doi:10.1007/s00134-013-3451-5.

- [11]. Xu H, Reynolds MM, Cook KE, Evans AS, Toscano JP, 2-Hydroxy-5-nitrobenzyl as a diazeniumdiolate protecting group: Application in no-releasing polymers with enhanced biocompatibility, *Org. Lett* 10 (2008) 4593–4596. doi:10.1021/ol801883f. [PubMed: 18811172]
- [12]. Amoako KA, Cook KE, Nitric oxide-generating silicone as a blood-contacting biomaterial, *ASAIO J* 57 (2011) 539–544. doi:10.1016/j.biotechadv.2011.08.021. Secreted. [PubMed: 22036723]
- [13]. Amoako KA, Montoya PJ, Major TC, Suhaib AB, Handa H, Brant DO, Meyerhoff ME, Bartlett RH, Cook KE, Fabrication and in vivo thrombogenicity testing of nitric oxide generating artificial lungs, *J. Biomed. Mater. Res. Part A* 101 (2013) 3511–3519. doi:10.1002/jbm.a.34655.
- [14]. Gupta S, Amoako KA, Suhaib A, Cook KE, Multi-Modal, Surface-Focused Anticoagulation Using Poly-2-methoxyethylacrylate Polymer Grafts and Surface Nitric Oxide Release, *Adv. Mater. Interfaces* 1 (2014). doi:10.1002/admi.201400012.
- [15]. Brisbois EJ, Handa H, Major TC, Bartlett RH, Meyerhoff ME, Long-term nitric oxide release and elevated temperature stability with S-nitroso-N-acetylpenicillamine (SNAP)-doped Elast-eon E2As polymer, *Biomaterials* 34 (2013) 6957–6966. doi:10.1016/j.biomaterials.2013.05.063. [PubMed: 23777908]
- [16]. Brisbois EJ, Major TC, Goudie MJ, Bartlett RH, Meyerhoff ME, Handa H, Improved hemocompatibility of silicone rubber extracorporeal tubing via solvent swelling-impregnation of S-nitroso-N-acetylpenicillamine (SNAP) and evaluation in rabbit thrombogenicity model, *Acta Biomater* 37 (2016) 111–119. doi:10.1016/j.actbio.2016.04.025. [PubMed: 27095484]
- [17]. Frost MC, Reynolds MM, Meyerhoff ME, Polymers incorporating nitric oxide releasing/generating substances for improved biocompatibility of blood-contacting medical devices, *Biomaterials* 26 (2005) 1685–1693. doi:10.1016/j.biomaterials.2004.06.006. [PubMed: 15576142]
- [18]. Brisbois EJ, Major TC, Goudie MJ, Meyerhoff ME, Bartlett RH, Handa H, Attenuation of thrombosis and bacterial infection using dual function nitric oxide releasing central venous catheters in a 9 day rabbit model, *Acta Biomater* (2016). doi:10.1016/j.actbio.2016.08.009.
- [19]. Vaughn MW, Kuo L, Liao JC, Estimation of nitric oxide production and reaction rates in tissue by use of mathematical model, *Am. J. Physiology* 43 (1998) H2163 <http://www.ncbi.nlm.nih.gov/pubmed/9134920>.
- [20]. Major TC, Brant DO, Burney CP, Amoako K. a., Annich GM, Meyerhoff ME, Handa H, Bartlett RH, The hemocompatibility of a nitric oxide generating polymer that catalyzes S-nitrosothiol decomposition in an extracorporeal circulation model, *Biomaterials* 32 (2011) 5957–5969. doi: 10.1016/j.biomaterials.2011.03.036. [PubMed: 21696821]
- [21]. Fleser PS, Nuthakki VK, Malinzak LE, Callahan RE, Seymour ML, Reynolds MM, Merz SI, Meyerhoff ME, Bendick PJ, Zelenock GB, Shanley CJ, Nitric oxide-releasing biopolymers inhibit thrombus formation in a sheep model of arteriovenous bridge grafts, *J. Vasc. Surg* 40 (2004) 803–811. doi:10.1016/j.jvs.2004.07.007. [PubMed: 15472611]
- [22]. Handa H, Major TC, Brisbois EJ, Amoako KA, Meyerhoff ME, Bartlett RH, Hemocompatibility comparison of biomedical grade polymers using rabbit thrombogenicity model for preparing nonthrombogenic nitric oxide releasing surfaces, *J. Mater. Chem. B* 2 (2014) 1059–1067. doi: 10.1039/c3tb21771j. [PubMed: 24634777]
- [23]. Skoog DJ, Pohlmann JR, Demos DS, Scipione CN, Iyengar A, Schewe RE, Suhaib AB, Koch KL, Cook KE, Fourteen Day in Vivo Testing of a Compliant Thoracic Artificial Lung, *ASAIO J* 63 (2017) 644–649. doi:10.1097/MAT.0000000000000627. [PubMed: 28719441]
- [24]. Cook KE, Perlman CE, Seipelt R, Backer CL, Mavroudis C, Mockrost LF, Hemodynamic and gas transfer properties of a compliant thoracic artificial lung., *ASAIO J* 51 (2005) 404–411. doi: 10.1097/01.mat.0000169707.72242.8f. [PubMed: 16156307]
- [25]. Serikov VB, Jerome EH, Noninvasive measurements of cardiac output in sheep: An improved thermometry method, *Med. Eng. Phys* 19 (1997) 618–629. doi:10.1016/S1350-4533(97)00021-0. [PubMed: 9457695]

- [26]. Evans W, Capelle SC, Edelstone DI, Lack of a critical cardiac output and critical systemic oxygen delivery during low cardiac output in the third trimester in the pregnant sheep, *Am. J. Obstet. Gynecol* 175 (1996) 222–228. doi:10.1016/S0002-9378(96)70279-X. [PubMed: 8694056]
- [27]. Cripps CM, Rapid method for the estimation of plasma haemoglobin levels, *J. Clin. Pathol* 21 (1968) 110–112. doi:10.1136/jcp.21.1.110. [PubMed: 5697326]
- [28]. Sato H, Griffith GW, Hall CM, Toomasian JM, Hirschl RB, Bartlett RH, Cook KE, Seven-Day Artificial Lung Testing in an In-Parallel Configuration, *Ann. Thorac. Surg* 84 (2007) 988–994. doi:10.1016/j.athoracsur.2007.03.016. [PubMed: 17720415]
- [29]. Sato H, Hall CM, Lafayette NG, Pohlmann JR, Padiyar N, Toomasian JM, Haft JW, Cook KE, Thirty-Day In-Parallel Artificial Lung Testing in Sheep, *Ann. Thorac. Surg* 84 (2007) 1136–1143. doi:10.1016/j.athoracsur.2007.05.051. [PubMed: 17888959]
- [30]. Menzies PI, Boermans H, Hoff B, Durzi T, Langs L, Survey of the status of copper, interacting minerals, and vitamin E levels in the livers of sheep in Ontario, *Can. Vet. J* 44 (2003) 898–906. [PubMed: 14664352]
- [31]. Rauch ED, Stammers AH, Mejak BL, Vang SN, Viessman TW, The effects of nitric oxide on coagulation during simulated extracorporeal membrane oxygenation., *J. Extra. Corpor. Technol* 32 (2000) 214–219. [PubMed: 11194058]
- [32]. Lantvit SM, Barrett BJ, Reynolds MM, Nitric oxide releasing material adsorbs more fibrinogen, *J. Biomed. Mater. Res. - Part A* 101 (2013) 3201–3210. doi:10.1002/jbm.a.34627.
- [33]. Major TC, Brant DO, Reynolds MM, Bartlett RH, Meyerhoff ME, Handa H, Annich GM, The attenuation of platelet and monocyte activation in a rabbit model of extracorporeal circulation by a nitric oxide releasing polymer, *Biomaterials* 31 (2010) 2736–2745. doi:10.1016/j.biomaterials.2009.12.028. [PubMed: 20042236]
- [34]. Mockros L, Leonard R, Compact Cross-Flow Tubular Oxygenators, *Trans. Am. Soc. Artif. Intern. Organs* 31 (1985) 628–633.
- [35]. Cook KE, Makarewicz AJ, Backer CL, Mockros LF, Przybylo HJ, Crawford SE, Hernandez JM, Leonard RJ, Mavroudis C, Testing of an intrathoracic artificial lung in a pig model., *ASAIO J* 42 (1996) M604–9. [PubMed: 8944952]
- [36]. Linder MC, Hazegh-Azam M, Copper biochemistry and molecular biology, *Am. J. Clin. Nutr* 63 (1996) 797–811.
- [37]. Chen Z, Meng H, Xing G, Chen C, Zhao Y, Jia G, Wang T, Yuan H, Ye C, Zhao F, Chai Z, Zhu C, Fang X, Ma B, Wan L, Acute toxicological effects of copper nanoparticles in vivo, *Toxicol. Lett* 163 (2006) 109–120. doi:10.1016/j.toxlet.2005.10.003. [PubMed: 16289865]
- [38]. Borkow G, Safety of using copper oxide in medical devices and consumer products, *Curr. Chem. Biol* 6 (2012) 86–92. <http://www.scopus.com/inward/record.url?eid=2-s2.0-84860301309&partnerID=40&md5=4f9b97ecab736ec9d28fe0c2e6b6f9d8>.
- [39]. Bremner I, Manifestations of copper excess, *Am. J. Clin. Nutr* 67 (1998).
- [40]. Dede S, Deger Y, Deger S, Serum Copper, Zinc, and Calcium Concentrations in Lice-Infested Sheep, *Biol. Trace Elem. Res* 88 (2002) 87–90. doi:10.1385/BTER:88:1:87. [PubMed: 12117268]
- [41]. Theil EC, Calvert KT, The effect of copper excess on iron metabolism in sheep, *J. Biochem* 170 (1978) 137–43. <http://www.pubmedcentral.nih.gov/articlerender.fcgi?artid=1183870&tool=pmcentrez&rendertype=abstract>.
- [42]. Buck WB, Sharma RM, Copper Toxicity in Sheep, *Iowa State Univ. Vet* 31 (1969) 4–8.
- [43]. Mohammed A, Campbell M, Youssef FG, Serum copper and haematological values of sheep of different physiological stages in the dry and wet seasons of central trinidad, *Vet. Med. Int* 2014 (2014). doi:10.1155/2014/972074.
- [44]. Wang YB, Shi KH, Jiang HL, Gong YK, Significantly reduced adsorption and activation of blood components in a membrane oxygenator system coated with crosslinkable zwitterionic copolymer, *Acta Biomater* 40 (2016) 153–161. doi:10.1016/j.actbio.2016.02.036. [PubMed: 26969525]
- [45]. Pieri M, Turla OG, Calabrò MG, Ruggeri L, Agracheva N, Zangrillo A, Pappalardo F, A new phosphorylcholine-coated polymethylpentene oxygenator for extracorporeal membrane

oxygenation: A preliminary experience, *Perfus. (United Kingdom)* 28 (2013) 132–137. doi: 10.1177/0267659112469642.

- [46]. Teman NR, Demos DS, Bryner BS, Faliks B, Jahangir EM, Mazur DE, Rojas-Pena A, Bartlett RH, Haft JW, In vivo testing of a novel blood pump for short-term extracorporeal life support, *Ann. Thorac. Surg* 98 (2014) 97–102. doi:10.1016/j.athoracsur.2014.04.027. [PubMed: 24856794]
- [47]. Skrzypchak AM, Lafayette NG, Bartlett RH, Zhou Z, Frost MC, Meyerhoff ME, Reynolds MM, Annich GM, Effect of varying nitric oxide release to prevent platelet consumption and preserve platelet function in an in vivo model of extracorporeal circulation, *Perfusion* 22 (2007) 193–200. doi:10.1177/0267659107080877. [PubMed: 18018399]

Statement of Significance

In artificial lungs, the large, densely-packed blood contacting surface area of the hollow fiber bundle is critical for gas exchange but also creates rapid, surface-generated clot requiring significant anticoagulation. Monitoring of anticoagulation, thrombosis, and resultant complications has kept permanent respiratory support from becoming a clinical reality. In this study, we use a hollow fiber material that generates nitric oxide (NO) to prevent platelet activation at the blood contacting surface. This material is tested in vivo in a miniature artificial lung and compared against the clinical standard. Results indicated significantly reduced clot formation. Surface-focused anticoagulation like this should reduce complication rates and allow for permanent respiratory support by extending the functional lifespan of artificial lungs and can further be applied to other medical devices.

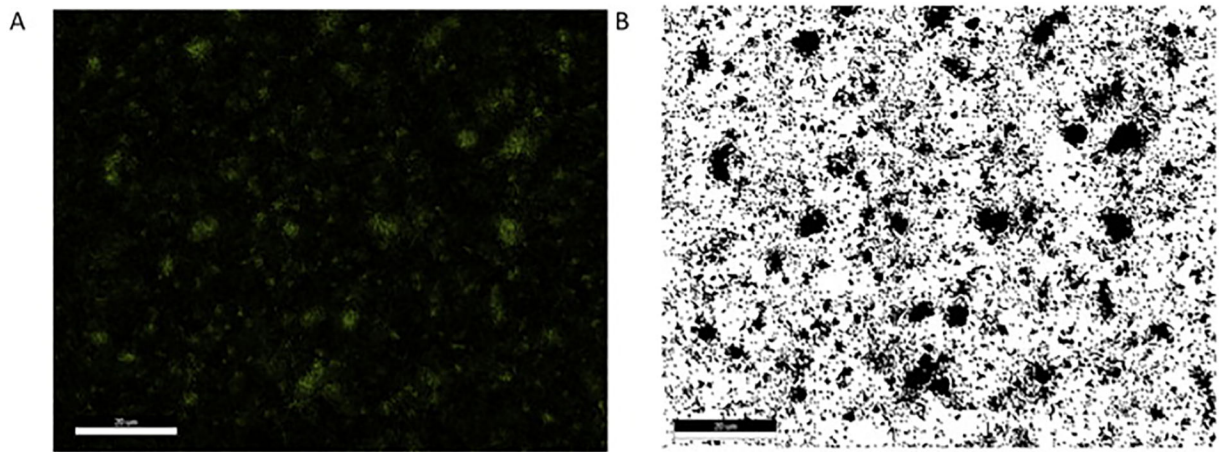


Figure 1. Energy dispersive microscopy is used to characterize the surface of Cu-PDMS fibers for copper exposed on the surface (A). Then, the image is converted to binary (B) and then all of the pixels representing copper are counted using ImageJ. Scale Bar 20 μm .

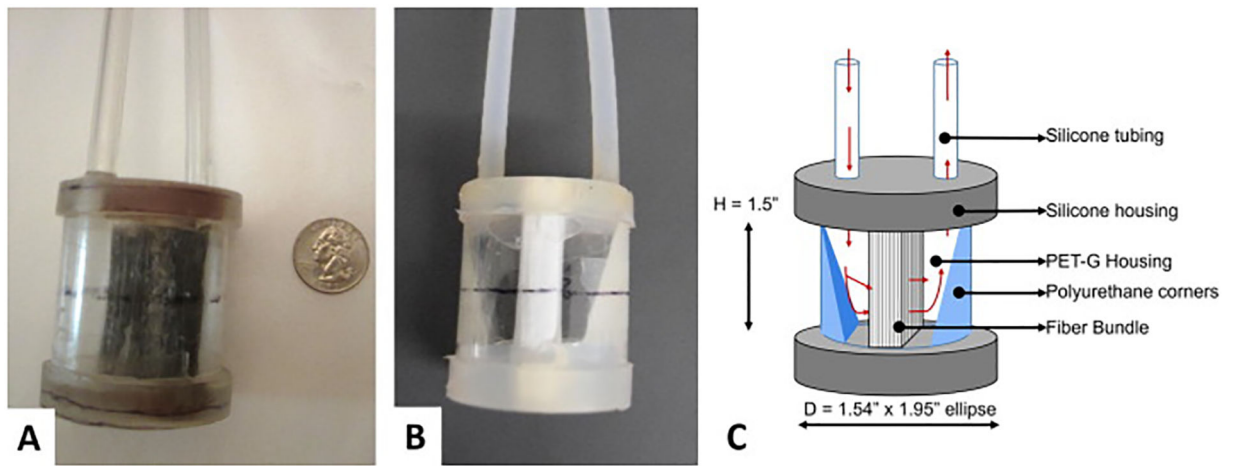


Figure 2.
A Cu-PDMS (right) and a PMP (left) miniature artificial lung.

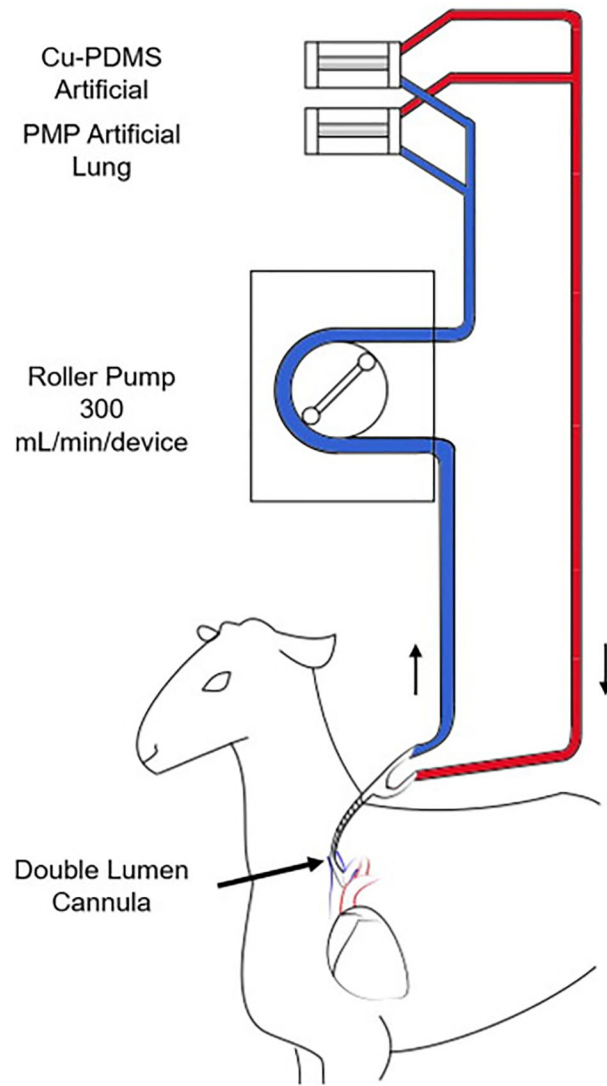


Figure 3. VV-ECMO circuit connecting a Cu-PDMS and a PMP device in parallel in a sheep model. The experimental timeline is as follows: T=0 Baseline samples; T=2 Circuit attachment; T=6 Device attachment set 1; Device attachment set 2 for each experiment was at T=8, 13,72 and 72 hours.

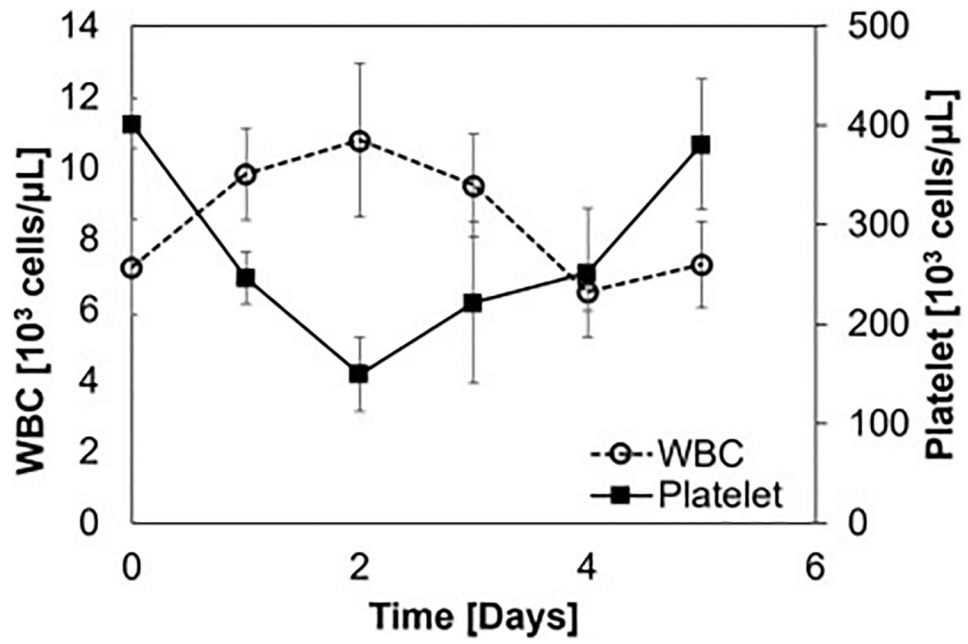


Figure 4. White blood cell count and platelet counts averaged over all subjects. Data are averaged over one day and presented with a standard deviation.

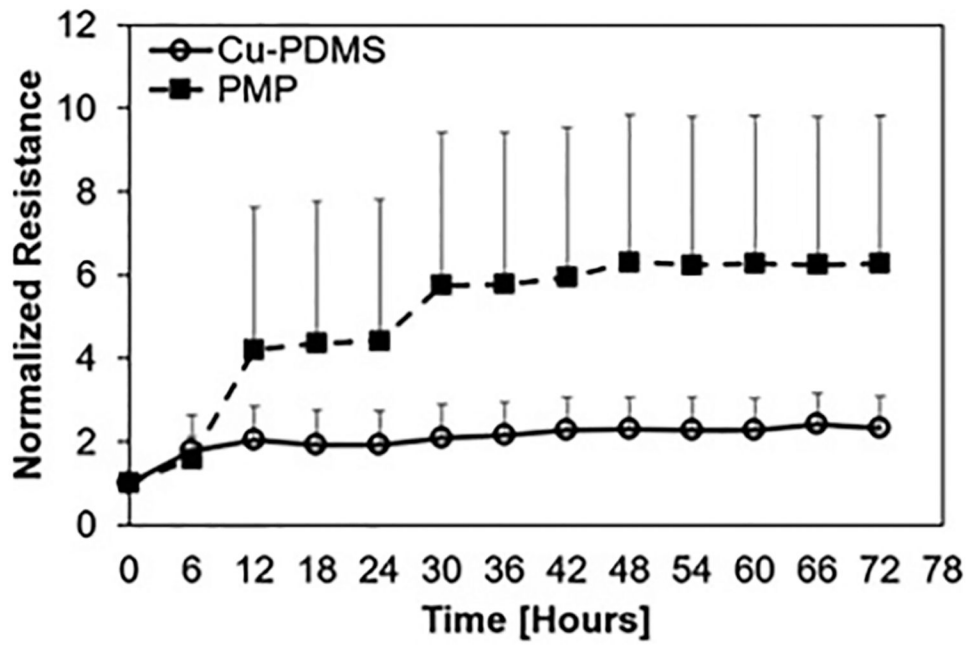


Figure 5. Normalized resistances to an averaged baseline show significant difference between Cu-PDMS and control devices. Data are averaged over 6-hour periods and presented with the standard deviation.

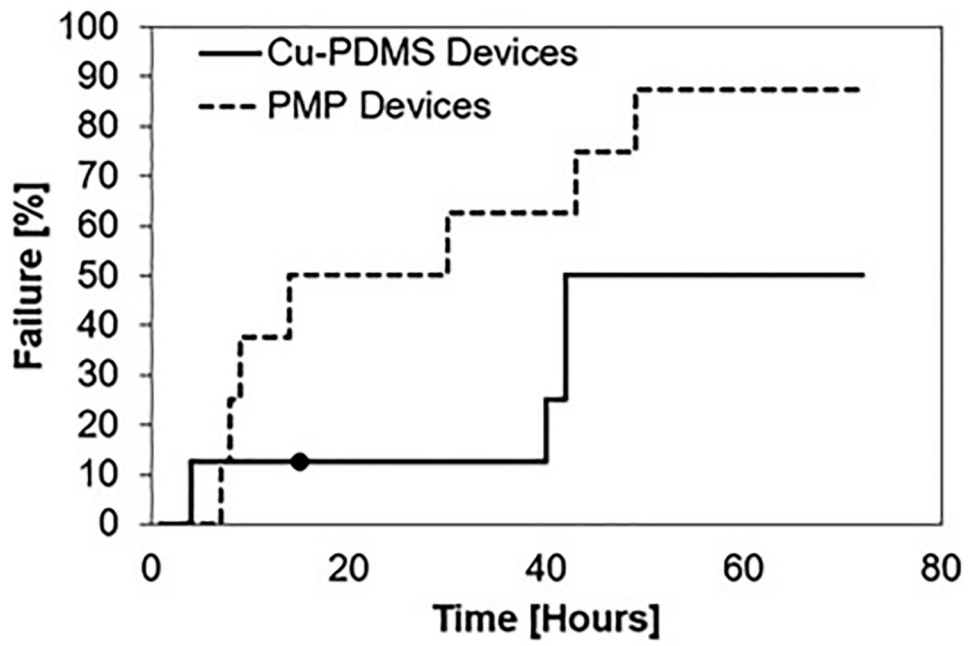


Figure 6.

Failure of Cu-PDMS and control PMP devices over 72 hours (N = 8). The ● represents a device that was removed before it was failed, data from this was used as a censored event in Kaplan-Meier survival analysis.

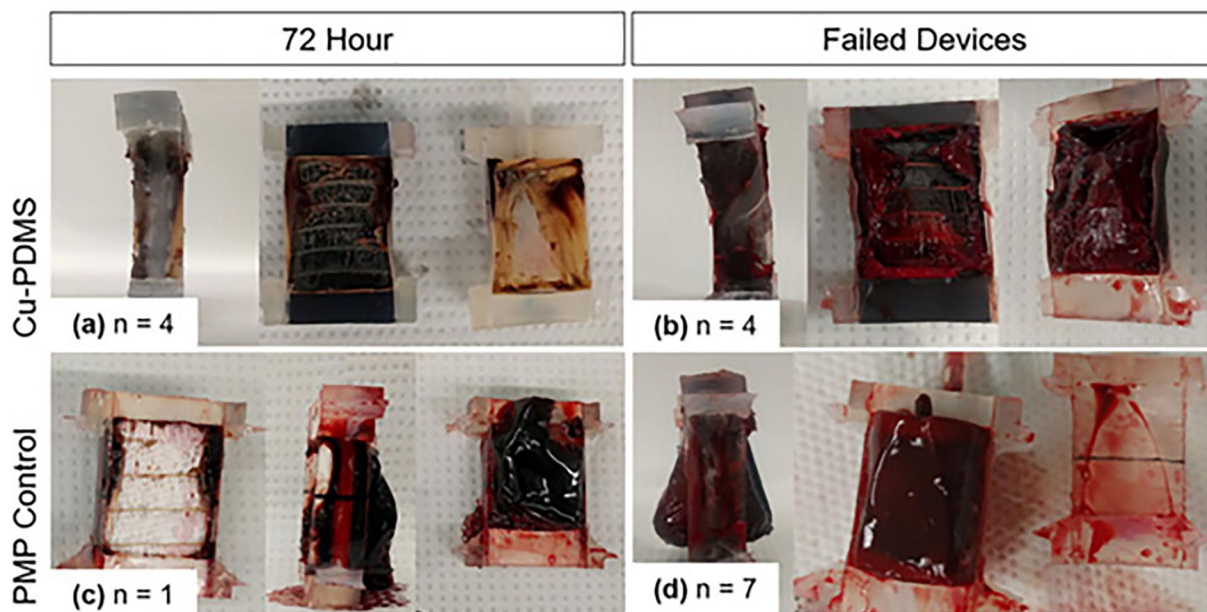


Figure 7.

Clot formation in lungs. As expected, devices that did not reach failure (a,c) have less clot than those that fail (b,d). (a) 50% of Cu-PDMS devices had black gas exchanging fibers visible and some white clot formation on the housing and edges. The other 50% of Cu-PDMS devices (b) failed. Only one PMP device (c) survived to 72 hours, and the rest (d) 87.5% failed and had clot originating from the fiber bundle, and no gas exchanging fibers can be seen.

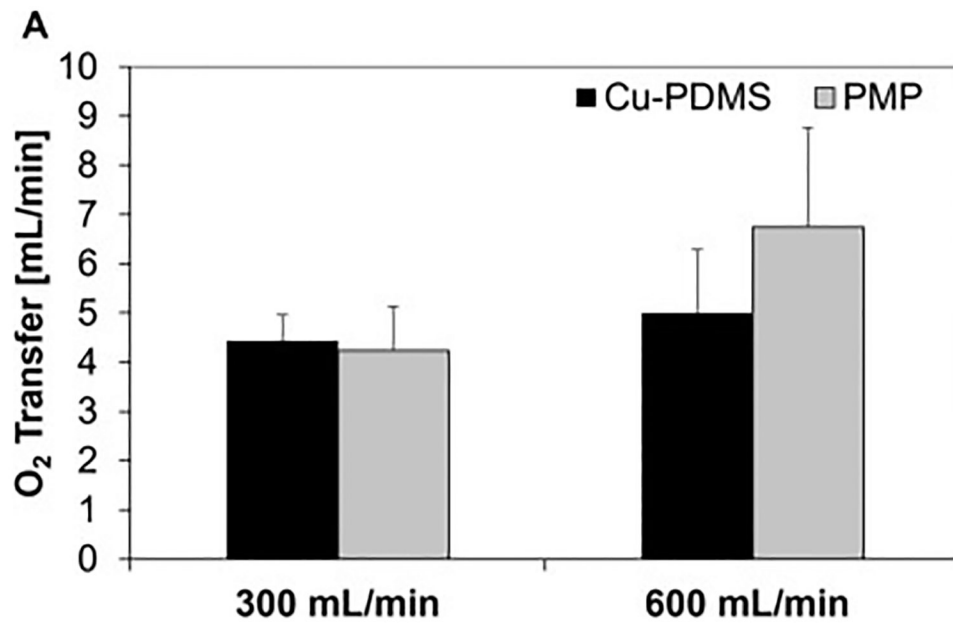


Figure 8. Oxygen transfer on D1 at 300 and 600 mL/min blood flow rate, and 600 and 1200 mL/min oxygen flow rate respectively (A). Data that had variable inlet conditions and high initial resistance were excluded.

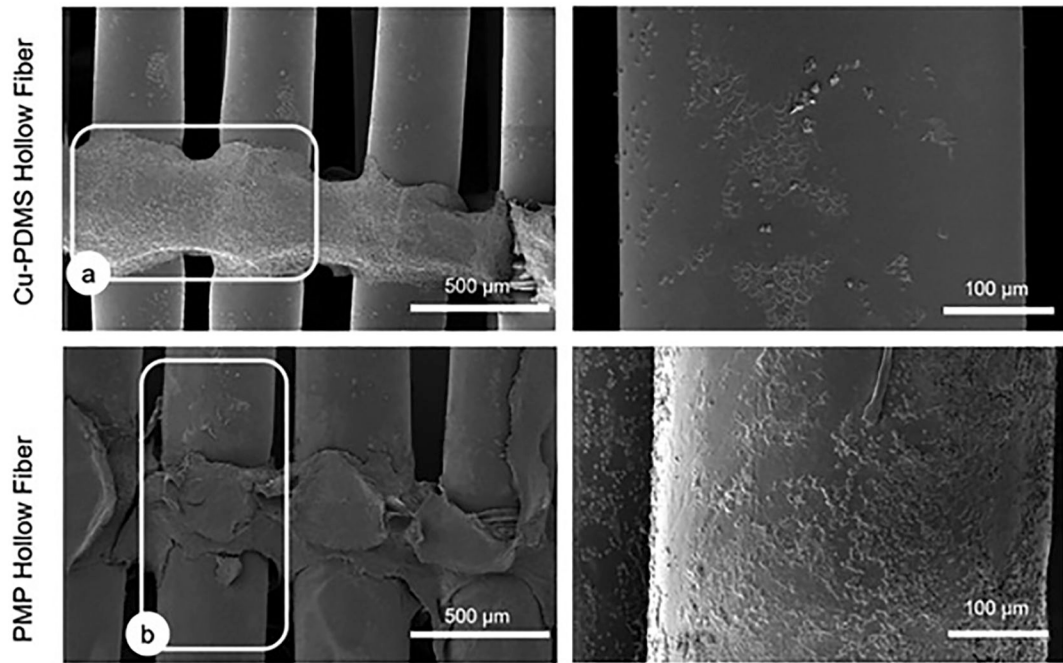


Figure 9. Representative SEM images of gas exchanging fibers and weaving fibers. (a) outlines a weaving fiber with pronounced protein deposition and (b) outlines a gas exchanging fiber. These are figures representing worst case scenarios, failed devices looking at the middle of the fiber bundle. (87.5% of the PMP devices and 50% of the Cu-PDMS devices)

Table 1.

Failure times (hours) for all devices attached to each sheep.

Sheep	Set 1		Set 2	
	Cu-PDMS	PMP	Cu-PDMS	PMP
1	-	-	72	29
2	14	13	-	-
3	4	7	42	6
4	72	6	40	49
5	72	72	42	43

Author Manuscript

Author Manuscript

Author Manuscript

Author Manuscript

Table 2

Oxygen exchange in mL/min/m² over three days, with number of devices in each group per day.

		D1	D2	D3
300 mL/min	Cu-PDMS	76±11	29±4	47±0
		N=5	N=3	N=1
	PMP	90±16	69±26	87±0
		N=5	N=4	N=1
600 mL/min	Cu-PDMS	93±17	41±9	24±0
		N=5	N=3	N=1
	PMP	106±30	103±39	111±0
		N=5	N=3	N=1

Author Manuscript

Author Manuscript

Author Manuscript

Author Manuscript